*The Plant Journal* (2004) **38**, 578–593 doi: 10.1111/j.1365-313X.2004.02069.x

# Cytokinin stimulates polyribosome loading of nuclear-encoded mRNAs for the plastid ATP synthase in etioplasts of *Lupinus luteus*: the complex accumulates in the inner-envelope membrane with the $CF_1$ moiety located towards the stromal space

**Irena Sherameti[1], Bationa Shahollari[1], Martin Landsberger[1,†], Martin Westermann[2], Galina Cherepneva[3], Victor Kusnetsov[3] and Ralf Oelmüller[1,*]**

[1]*Institut für Allgemeine Botanik und Pflanzenphysiologie, Friedrich-Schiller-Universität Jena, Dornburger Str. 159, D-07743 Jena, Germany,*

[2]*Institut für Ultrastrukturforschung des Klinikums der Friedrich-Schiller-Universität Jena, Ziegenmühlenweg 1, 07740 Jena, Germany, and*

[3]*Timiriazev Institute of Plant Physiology, Russian Academy of Sciences, ul. Botanicheskaya 35, Moscow 127276, Russia*

Received 5 November 2003; revised 6 January 2004; accepted 30 January 2004.

*For correspondence (fax +49 3641 949232; e-mail Ralf.Oelmueller@rz.uni-jena.de).

†Present address: AG Molekulare Kardiologie, Klinik für Innere Medizin B, Universität Greifswald, Friedrich-Loeffler-Strasse 23a, 17487 Greifswald, Germany.

**Summary**

**Three of the nine subunits of the plastid ATP synthase, including the subunit of the $CF_1$ moiety (gene *AtpC*), are encoded in the nucleus. Application of cytokinin to etiolated lupine seedlings induces polyribosome association of their mRNAs. This appears to be specific as no such regulation was observed for messages for three ribosomal proteins. Cytokinin-mediated polyribosome loading was also observed for the spinach *AtpC* message in etiolated transgenic tobacco seedlings. Analysis of various spinach *AtpC* mRNA derivatives uncovered that the 5′ untranslated region (5′ UTR) of this message is sufficient to direct polyribosome loading, and that sequences at the 3′ end of the *AtpC* 5′ UTR, including an UC-rich motif, are crucial for this regulation. The increase in polyribosome loading of the *AtpC* message correlated with an increased synthesis of the polypeptide. The subunit, together with the ATP synthase complex, accumulates in the inner-envelope membrane with the $CF_1$ moiety located towards the stromal space of the etioplast. These results suggest that cytokinin promotes accumulation of the ATP synthase in the inner-envelope membrane of lupine etioplasts by stimulating the translation efficiency of their nuclear-encoded messages.**

**Keywords: ATP synthase, cytokinin, envelope membrane, etioplast, polyribosome loading, 5′ untranslated region.**

## Introduction

The plastid ATP synthase is a membrane-bound complex, which couples ATP synthesis to a transmembrane proton transport (Jagendorf and Uribe, 1966). The enzyme consists of two domains, a membrane-integrated $F_0$ moiety, which is involved in the proton transport, and a water-soluble $F_1$ part, which carries the nucleotide-binding sites. The two parts are connected by a central stalk and probably by a second peripheral connection (cf. Junge *et al.*, 1997). Much of the information about the structure of ATP synthases – the number, localization and orientation of their subunits, and the function of the holocomplex – has been confirmed by X-ray crystallography (Abrahams *et al.*, 1994). ADP and $P_i$ is bound to the β-subunit of the $F_1$ moiety, and ATP is synthesized (cf. Boyer, 1997, references therein). The energy required to remove the ATP from the complex is provided by a rotation of the $CF_1$ complex. The central subunit functions as a stalk and pushes one pair of the α/β-trimer of the $CF_1$ moiety, with every movement being at 120° (Cross and Duncan, 1996; Noji *et al.*, 1997; Sabbert *et al.*, 1996, 1997). The most likely reason for this movement

 

is a response to protons rushing through the membrane-integral $CF_0$ stalk, although it is still not understood exactly how the two movements are coupled (cf. Junge *et al.*, 1997).

In photosynthetic eukaryotes, the plastid ATP synthase consists of nine subunits, three of them are encoded by the nuclear genes *AtpC*, *AtpD*, and *AtpG* (gene products: the subunits $\gamma$ and $\delta$ of the $CF_1$ moiety and $CF_0$II; cf. Herrmann *et al.*, 1991). Genes for the residual subunits reside in the organelle. Expression of the nuclear genes exhibits unusual features. For instance, the spinach *AtpC* gene contains all known *cis*-regulatory elements for its regulated expression in the vicinity of the transcription start site (Bolle *et al.*, 1996a). Apparently, the assembly of the CAAT box-binding complex appears to be crucial for transcription, and this process competes with a repressor polypeptide (Bezhani *et al.*, 2001; Kusnetsov *et al.*, 1999). In contrast, *AtpD* gene expression is strongly stimulated by an enhancer-like element located further upstream in the promoter, and corresponding elements are not present in the *AtpC* promoter (Bolle *et al.*, 1996a). In spinach, the transcript levels for the three nuclear-encoded subunits exhibit a coordinate diurnal regulation, while the protein levels remain constant (Oelmüller *et al.*, 1995). Thus, steady-state mRNA levels do not reflect the rates of protein synthesis of various ATP synthase subunits (cf. Bolle *et al.*, 1992; Herrmann *et al.*, 1991; Kusnetsov *et al.*, 1994, data shown here). This is particularly striking during the greening process of etiolated seedlings (Herrmann *et al.*, 1991), and was also observed for etiolated lupine or pumpkin cotyledons treated with phytohormones (Kusnetsov *et al.*, 1994, 1996). Furthermore, etiolated pumpkin or lupine seedlings contain high AtpC protein levels, and these levels increase only moderately in light in contrast to low steady-state *AtpC* mRNA levels in darkness, which are stimulated at least 10-fold by light (Oelmüller *et al.*, unpublished). This suggests the existence of additional regulatory processes operating between mRNA accumulation and protein synthesis. It has been reported that polyribosome loading of messages for photosynthesis proteins represents an efficient and rapid mechanism to adapt protein synthesis to environmental changes (cf. Petracek and Thompson, 2000). Therefore, we tested whether cytokinin controls polyribosome loading of the nuclear-encoded messages for the plastid ATP synthase subunits $\gamma$, $\delta$ and $CF_0$II. We found that this appears to be a general phenomenon as it was also observed in spinach and tobacco. For one of the messages, *AtpC* from spinach, we demonstrate that sequences within the 5′ untranslated region (5′ UTR) are sufficient to promote polyribosome loading in transgenic tobacco seedlings in response to cytokinin. Furthermore, an increase in polyribosome loading of the *AtpC* message correlated with an increase in protein synthesis. The complex accumulates in the inner-envelope membrane of lupine etioplasts with the $CF_1$ moiety located toward the stromal space.

## Results

Association of photosynthesis mRNAs with polyribosomes represents a rapid and efficient mechanism for acclimating photosynthesis gene expression to cell-internal and -external signals (Dickey *et al.*, 1998; Hansen *et al.*, 2001; Ling *et al.*, 2000; Petracek *et al.*, 1997, 1998, 2000; Sherameti *et al.*, 2002, and references therein). As we could not correlate changes in the steady-state mRNA levels of *AtpC*, *AtpD*, and *AtpG* with the rates of synthesis of the corresponding proteins (see Introduction; cf. Bolle *et al.*, 1996a; Herrmann *et al.*, 1991; Kusnetsov *et al.*, 1994), we tested whether polyribosome association is a possible target site for regulation. We isolated crude ribosomal fractions from etiolated lupine cotyledons which were treated with either cytokinin, abscisic acid, or water for 24 h. Polyribosome extracts with equal amounts of *AtpC*, *AtpD*, and *AtpG* messages (Figure 1a) were then layered on the top of a sucrose gradient. After centrifugation, the monoribosomes remained on the top of the gradient in the region of less than 20% sucrose, while polyribosomes were preferentially found at sucrose concentrations >35%, as measured by UV tracing at 254 nm and sucrose refractometry (cf. Dickey *et al.*, 1998, references therein; Sherameti *et al.*, 2002). Figure 1(b) demonstrates that significantly higher amounts of the *AtpC, AtpD*, and *AtpG* messages were polyribosome-associated after cytokinin treatment, while no significant effect was observed after the application of abscisic acid. We conclude that polyribosome loading of the three nuclear-encoded messages for the plastid ATP synthase in etiolated lupine cotyledons is influenced by cytokinin. As a control, we used a tubulin gene (Sherameti *et al.*, 2002) and found that this message did not respond to phytohormone treatments (Figure 1b). Abscisic acid treatments did not show measurable differences to the water control; thus, for the experiments shown below, only cytokinin was used. Finally, as a second control, we analyzed three messages for the ribosomal proteins rps13, rpl30, and rpl13b. They have been chosen because the steady-state mRNA levels of these messages increase after the application of cytokinin to etiolated lupine cotyledons, similar to those for *AtpC*, *AtpD*, and *AtpG* (Cherepneva *et al.*, 2003). However, in contrast to the results obtained for *AtpC*, *AtpD*, and *AtpG*, polyribosome loading of the messages for the ribosomal proteins is not altered after cytokinin application (Figure 2). Thus, the messages for the ribosomal proteins can also be used as controls, and demonstrate that the stimulation of polyribosome loading change after cytokinin application is not observed for all cytoplasmic mRNAs.

Figure 3(a) demonstrates that the steady-state *AtpC* mRNA level in etiolated lupine seedlings does not increase

measurably within 1.5 and 3 h after transfer of the cotyledons from water to cytokinin, while after 4.5 and 8 h, a significantly higher mRNA level could be detected. In contrast, cytokinin-mediated stimulation of polyribosome loading of the *AtpC* message was already detectable after 90 min, and this effect is not different from the results obtained 8 h after the phytohormone application (Figure 3b). *In vivo* labeling experiments with etiolated lupine cotyledons and subsequent immunoprecipitation of the AtpC protein revealed that cytokinin stimulates AtpC synthesis and that this effect is clearly detectable 90 min after the application of the phytohormone (Figure 3c). The amount of antibodies used for these studies are not limiting for the immunoprecipitation as demonstrated by the experiment shown in Figure 3(d). This suggests that the effect of cytokinin on AtpC protein synthesis is mediated by a more efficient translation of its message rather than an increase in the steady-state mRNA level.

To test whether this regulation is also observed for ATP synthase messages in other species and to identify sequences which are possibly involved in phytohormone-mediated polyribosome loading, we analyzed transcripts deriving from a 5226-bp long spinach DNA fragment that contains the complete *AtpC* gene, including the two introns and 5′ and 3′ flanking sequences (1440 bp upstream of the transcription start site and 730 bp downstream of the stop codon) in transgenic tobacco. The transcripts were monitored with a probe covering the 5′ UTR plus the nucleotide sequence for the plastid-directing transit sequence (cf. Experimental procedures). Polyribosome association of the spinach *AtpC* message in transgenic tobacco seedlings was significantly stimulated by cytokinin (Figure 4).

Primer extension analysis uncovered that the 5′ UTR of *AtpC* comprises 173 bp (Bolle *et al.*, 1996a,b). To check whether the 5′ UTR is involved in polyribosome loading, we tested transgenic tobacco lines with a construct containing a −1874/+173-bp spinach *AtpC* fragment fused to the bacterial *uidA* gene. This spinach DNA fragment was chosen because it contains promoter elements which direct high level of expression in tobacco (Bolle *et al.*, 1996a). Three independent experiments with RNA from three independent primary transformants revealed that the spinach messages become polyribosome-associated in transgenic tobacco seedlings in a cytokinin-dependent manner (Figure 5). As a control, we used transgenic tobacco seedlings in which a gene fusion generating *uidA* transcripts without the *AtpC* 5′ UTR was expressed under the control of

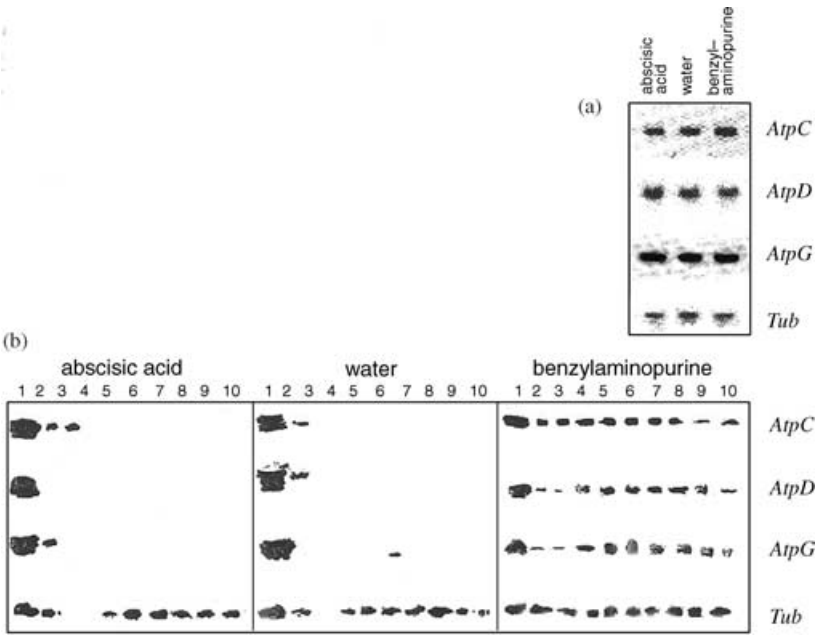


**Figure 1.** Polyribosome profiles for the *AtpC*, *AtpD*, and *AtpG* messages from etiolated lupine cotyledons, which were either non-treated (water), or treated with abscisic acid or benzylaminopurine.
(a) Northern analysis for *AtpC*, *AtpD*, and *AtpG* from RNA isolated from crude ribosomal preparations of etiolated lupine cotyledons. Crude ribosomal extracts with equal levels of *AtpC*, *AtpD*, and *AtpG* messages were loaded per lane (a) and on top of the sucrose gradients (b). *Tub*, hybridization with a tubulin probe to confirm equal loading.
(b) Polyribosome profiles for *AtpC*, *AtpD*, *AtpG*, and *Tub* messages from lupine cotyledons, which were either non-treated (water), or treated with abscisic acid or benzylaminopurine. After sucrose gradient centrifugations and RNA extraction from the individual fractions, Northern hybridization was performed with the respective probes (cf. Experimental procedures). Numbers refer to 1-ml fractions from top to bottom of the sucrose gradient (20–60%). Representative of five independent experiments. The Northern hybridizations are overexposed to detect also low levels of messages in the individual fractions.
(c) Quantification of the data shown in (b). The signals were quantified by the phosphorimager, and those for one gradient were set as 100%. The value for each fraction is expressed as percentage of the total gradient. Bars represent SEs, based on five independent experiments.

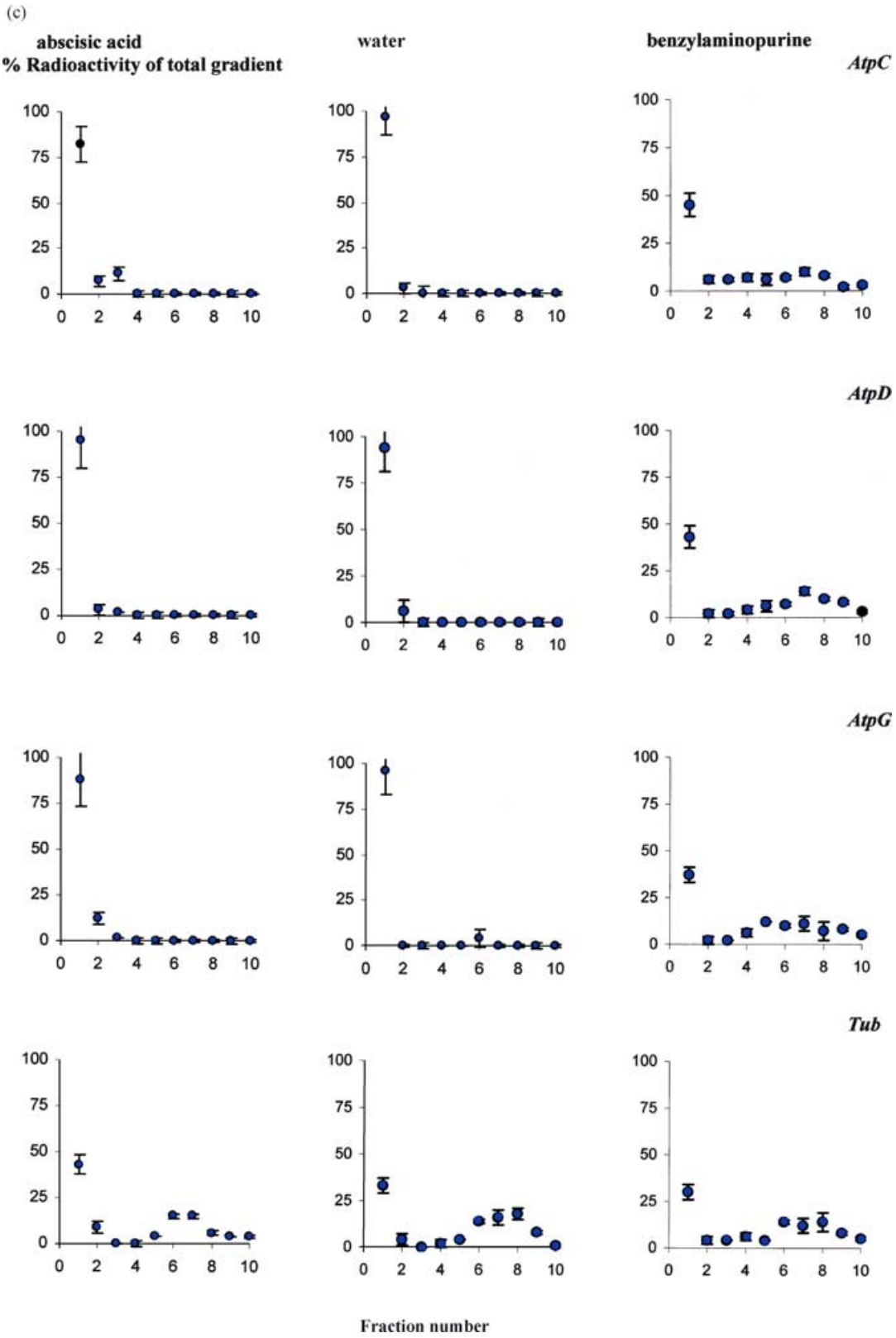


**Figure 1.** continued

the 35S RNA CaMV promoter (Figure 5). No obvious cytokinin effect could be detected. Thus, the 5′ UTR of the spinach *AtpC* message at the 5′ end of the *uidA* message is sufficient to direct cytokinin-dependent polyribosome loading in tobacco. Furthermore, this experiment also excludes the possibility of unspecific polyribosome loading of cytoplasmic messages after cytokinin application to etiolated seedlings.

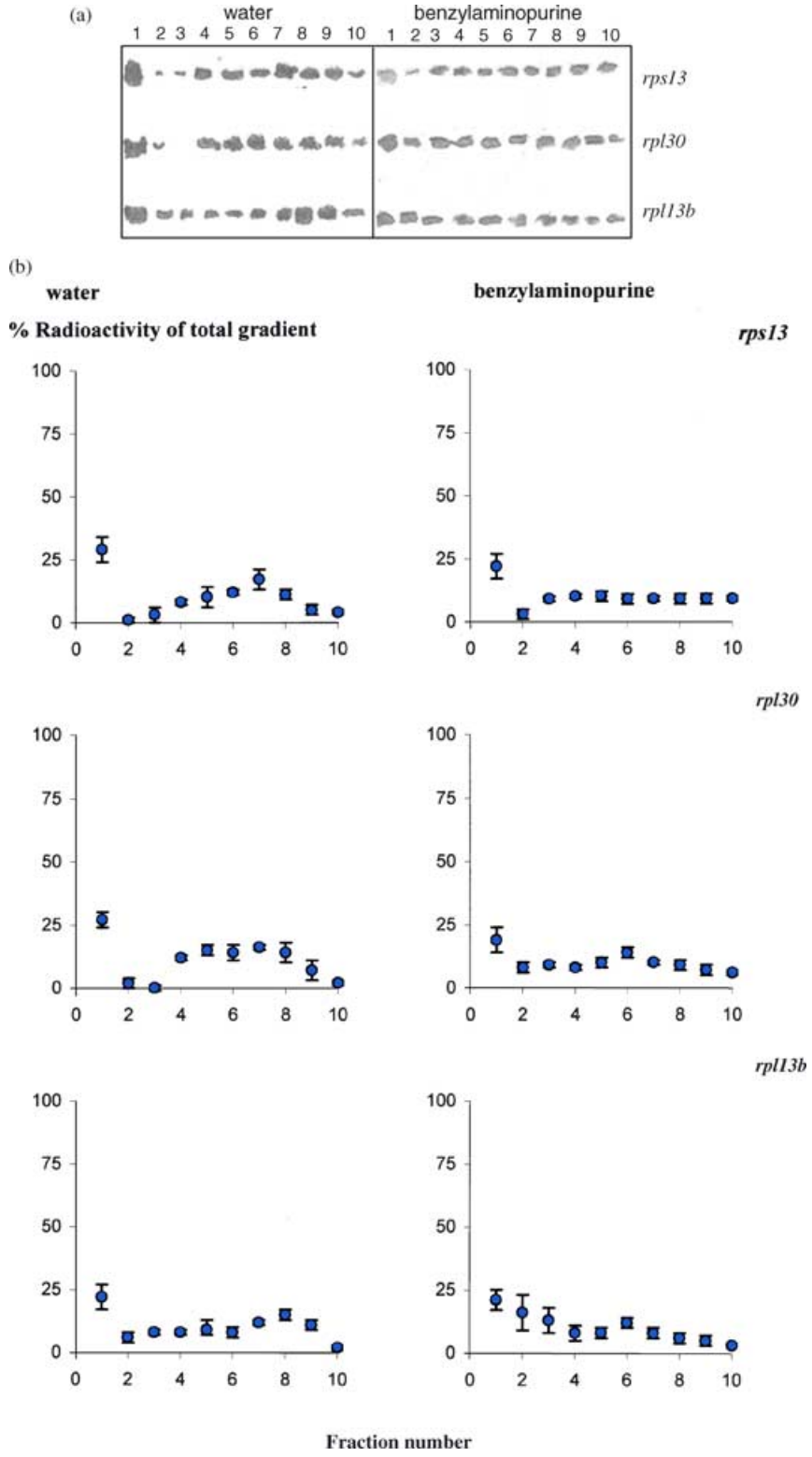


**Figure 2.** The effect of benzylaminopurine on the polyribosome profiles for rps13, rpl30, and rpl13b.
(a) Polyribosome profiles for *rps13*, *rpl30*, and *rpl13b* messages from etiolated lupine cotyledons, which were either non-treated (water), or treated with benzylaminopurine. After sucrose gradient centrifugations and RNA extraction from the individual fractions, Northern hybridizations were performed for RNA identification and quantification (cf. Experimental procedures). Numbers refer to 1-ml fractions from top to bottom of the sucrose gradient (20–60%). Representative of four independent experiments. The Northern hybridizations are overexposed to detect also low levels of messages in the individual fractions.
(b) Quantification of the data. The signals were quantified by the phosphorimager and those for one gradient were set as 100%. The value for each fraction is expressed as percentage of the total gradient. Bars represent SEs, based on four independent experiments.

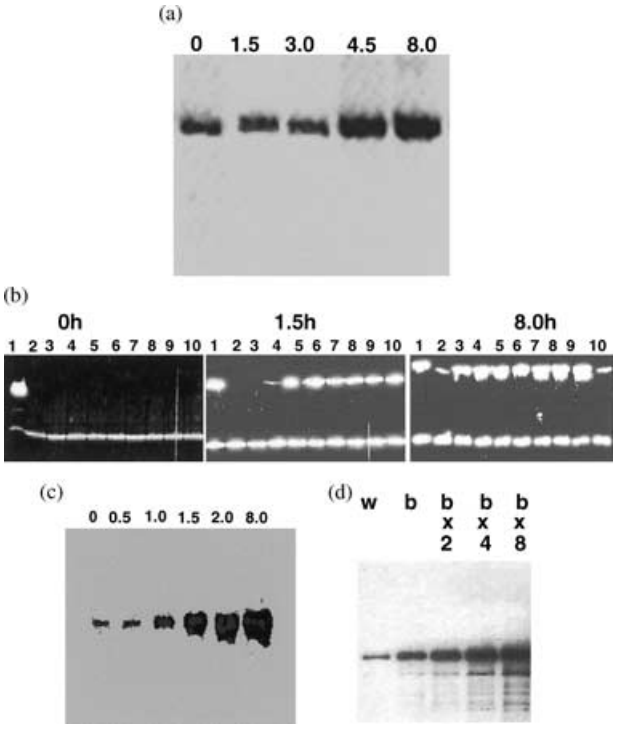


**Figure 3.** Cytokinin-induced polyribosome loading of the *AtpC* message correlates with an increase in AtpC protein synthesis in etiolated lupine cotyledons.
(a) Northern analysis for *AtpC*. Numbers refer to hours after cytokinin application.
(b) Polyribosome profile before (0 h), 1.5, and 8.0 h after cytokinin application. For experimental details, cf. legend to Figure 2.
(c) Immunoprecipitation of radiolabeled AtpC protein. Numbers refer to hours after cytokinin application.
(d) The amount of the AtpC-specific antiserum is not limiting for the analysis. Nine μl of purified antiserum was used for the immunoprecipitation of radiolabeled AtpC protein from water control extracts (w) and extracts from lupine cotyledons treated with benzylaminopurine (b). Two, four, or eight times of the latter extract was used for immunoprecipitations with the same amount of antiserum.

For the experiments described below, Northern analyses were not sensitive enough to detect *uidA* transcript levels in the individual gradient fractions. Therefore, we used the reverse transcriptase (RT)-PCR technique (Bolle *et al.*, 1996b; cf. Experimental procedures). The PCR reactions were performed with a primer pair that amplifies two *uidA* fragments: a 500-bp fragment, derived from the *uidA* cDNA generated from the mRNA under study, as well as a 300-bp *uidA* fragment, which was added to the reaction as a control. The latter fragment contains an *uidA* internal deletion (cf. Experimental procedures). Figure 5(b) demonstrates that the primer pair and the conditions used for the RT-PCR give results which are comparable to those obtained by conventional Northern analyses (Figure 5a).

Cytokinin-mediated polyribosome loading of chimeric *uidA* messages is still detectable in etiolated tobacco seedlings with the *AtpC* fragment −73/+173, although the overall transcript level is relatively low because of the short promoter region (Figure 6). 3′-Deletions of the spinach *AtpC* 5′-UTR from +173 to +133 or +103 severely reduced the extent of polyribosome loading after cytokinin application, although the shortest segment still gave rise to messages which responded to cytokinin. No transgene messages could be detected in plants harboring the −73/+7 construct, presumably because of the lack of transcription of the transgene (Bolle *et al.*, 1996b).

Previously, we have demonstrated that a CT-rich sequence motif found at position −106/+117, relative to the transcription start site of *AtpC*, is essential for the expression of *AtpC::uidA* gene fusion constructs in transgenic tobacco (Bolle *et al.*, 1996a,b). This region was investigated in more details because identical or comparable sequence elements are present in many photosynthesis gene 5′ UTRs (Bolle *et al.*, 1996b). Site-directed mutagenesis within this region uncovered that the integrity of the UUUCUCUCUCCU motif (+106/+117) in the *AtpC* message is important for proper polyribosome loading. Two mutant messages in which this sequence was changed to either AAAGAGAGACCU (M1) or GAUGUGACUCCU (M2) in the context of the full-length 5′ UTR barely showed any polyribosome loading after cytokinin application, although sufficient mRNA could be detected on top of the sucrose gradients (Figure 6). The UC-rich sequence motif is present in many plant 5′ UTRs, and appears to be conserved in genes which respond to signals, such as light, phytohormones, or developmental programs (Databank searches not shown). Taken together, these results suggest that the proper 3′ end of the 5′ UTR and the UC-rich sequence motif are essential for cytokinin-mediated polyribosome loading of the spinach *AtpC* message in etiolated tobacco seedlings (cf. Discussion).

The stimulatory effect of cytokinin on polyribosome loading of the nuclear-encoded messages for the plastid ATP synthase in etiolated *Lupinus luteus* cotyledons correlated with an increase in the protein level for several subunits of this complex (AtpA-AtpC, AtpE (subunits α, β, γ, and ε of the $CF_1$ moiety); Figure 7). The same was observed for the protochlorophyllide-oxidoreductase (Figure 7; Kusnetsov *et al.*, 1998). Although different systems of reference are used for the polyribosome experiments (Figure 1) and the Western analysis (Figure 7), and thus quantitative comparison of the data is difficult, it appears that the increase in the protein is less dramatic than the change in the polyribosome loading. No regulation was observed for 33-kDa protein of photosystem II (PsbO), while light-harvesting chlorophyll-*a/b*-binding protein (Lhc) was not detectable in etiolated material (Figure 7).

The results obtained so far raises the question that where are the subunits of the ATP synthase located in lupine etioplasts. Western analysis demonstrated that several subunits of the ATP synthase are present in the membrane

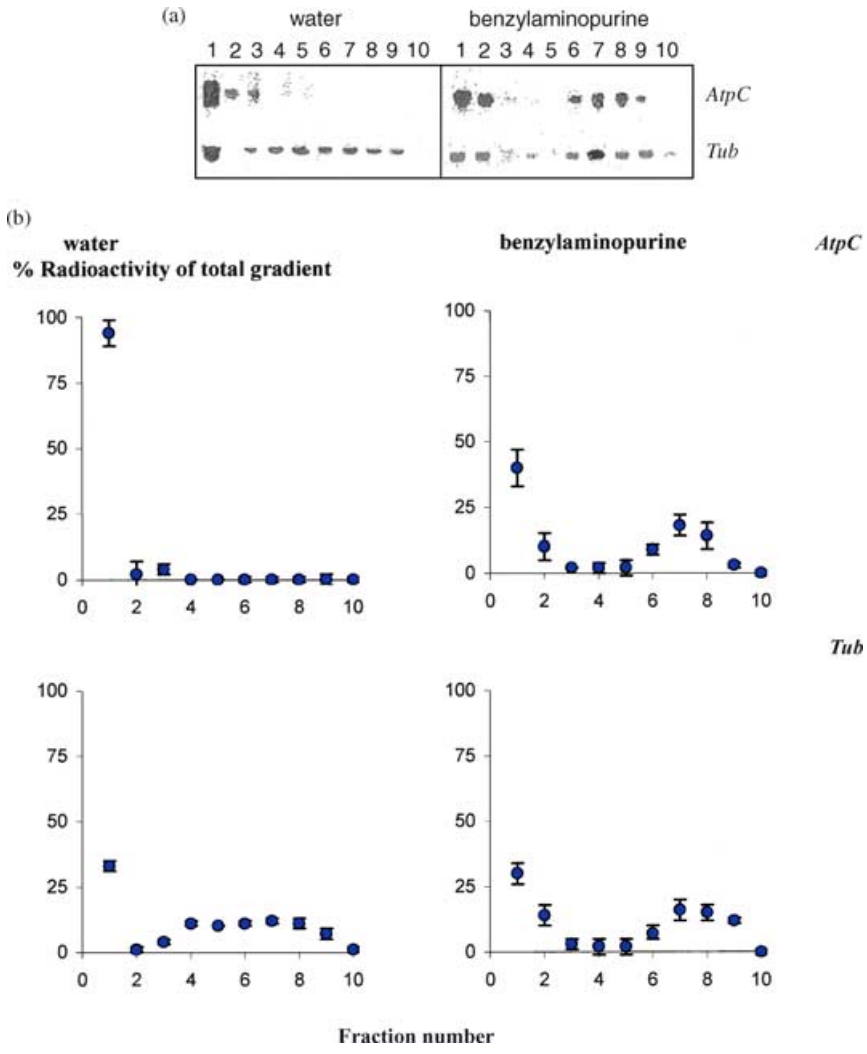


**Figure 4.** Polyribosome profiles for the *AtpC* and *Tub* messages in etiolated tobacco seedlings as affected by benzylaminopurine.
(a) Polyribosome profiles for the spinach *AtpC* message in etiolated transgenic tobacco seedlings which were either kept on water, or were treated with benzylaminopurine. After sucrose gradient centrifugations and RNA extraction from the individual fractions, Northern hybridization was performed with a spinach *AtpC*-specific DNA fragment or the tubulin (*Tub*) gene (cf. Experimental procedures). Numbers refer to 1-ml fractions from top to bottom of the sucrose gradient (20–60%). Representative of three independent experiments.
(b) Quantification of the data. The signals were quantified by the phosphorimager and those for one gradient were set as 100%. The value for each fraction is expressed as percentage of the total gradient. Bars represent SEs, based on three independent experiments.

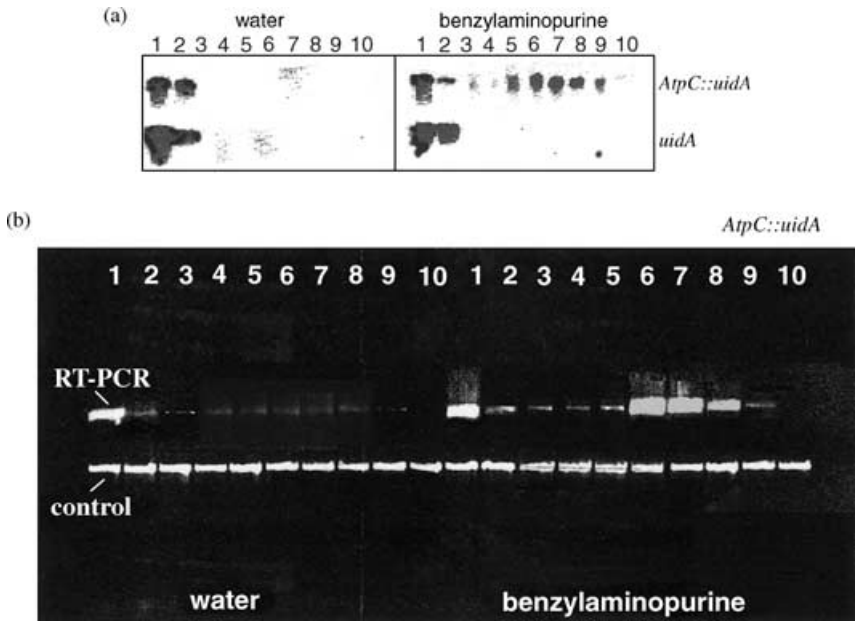


**Figure 5.** The effect of the spinach *AtpC* 5′ UTR on polyribosome loading of the *uidA* message.
(a) Polyribosome profiles of messages expressed from a chimeric construct of the spinach *AtpC*-1874/+173 region fused to the bacterial *uidA* gene (*AtpC::uidA*) or the bacterial *uidA* gene alone (*uidA*). Polyribosomes were isolated from etiolated transgenic tobacco seedlings, which were either kept on water or treated with benzylaminopurine. Numbers refer to 1-ml fractions from top to bottom of the sucrose gradient (20–60%). Representative of three independent experiments.
(b) Quantitative PCR for the *uidA* message (upper band, RT-PCR) from transgenic tobacco seedlings harboring the *AtpC::uidA* construct. Left: fractions 1–10 from the polyribosome profile of seedlings grown on water; right: fractions 1–10 from the polyribosome profile of seedlings treated with benzylaminopurine. The smaller PCR product represents controls for PCR reaction (cf. Experimental procedures). Representative for more than 10 independent experiments with RNA from three independent primary transformants.

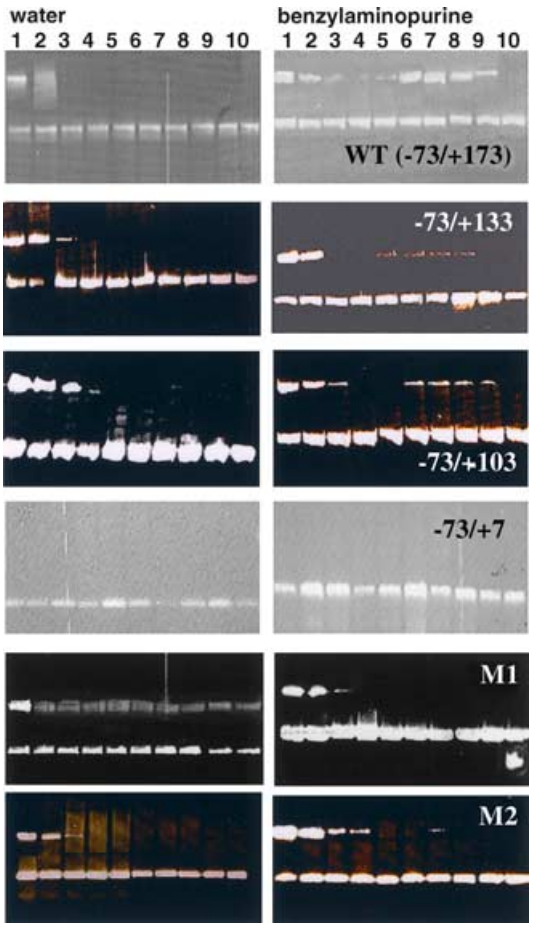


**Figure 6.** Polyribosome profiles for bacterial *uidA* messages with various 5′ extensions from the spinach *AtpC* gene in etiolated transgenic tobacco seedlings, which were either kept on water or treated with benzylaminopurine.
The spinach *AtpC*-derived 5′ extensions of the *uidA* messages are transcribed from the indicated constructs. M1 and M2 are mutants of the wild-type −73/+173 (cf. text). After sucrose gradient centrifugations and RNA extraction from the individual fractions, RT-PCR was performed with *uidA*-specific primers (cf. Experimental procedures). Numbers refer to 1-ml fractions from top to bottom of the sucrose gradient (20–60%). Representative of five independent experiments.

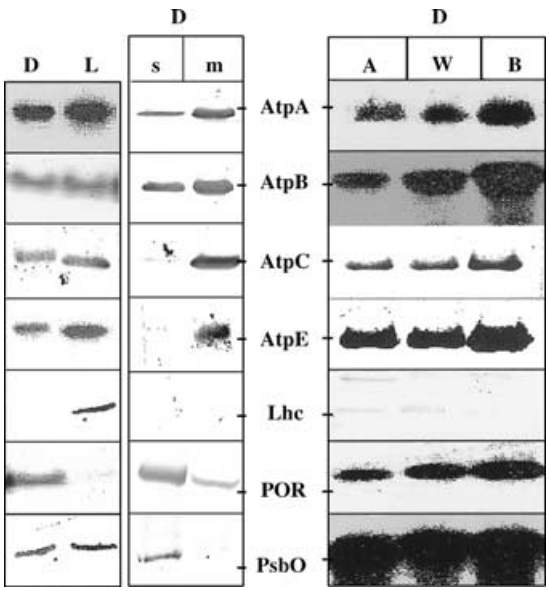


**Figure 7.** Plastid proteins as affected by abscisic acid and benzylaminopurine.
Western analysis with protein extracts from etiolated (D) or light-grown (L) lupine cotyledons, which were treated either with water (left two panels and lane W in right panel), or with abscisic acid or benzylaminopurine (A or B in right panel). s, m of middle panel: soluble and membrane-associated polypeptides from etiolated material, respectively. The antibodies recognize the polypeptides indicated between the panels. AtpA–C and AtpE: subunits α, β, γ, and ε of the $CF_1$ moiety of the plastid ATP synthase, respectively; Lhc, light-harvesting chlorophyll-*a/b*-binding protein; POR, protochlorophyllide-oxidoreductase; PsbO, 33 kDa protein of photosystem II. Representative of four independent analyses.

fraction of etioplasts, while only traces could be detected in the soluble fraction (Figure 7). Furthermore, if the membrane-associated proteins of purified etioplasts are separated on two-dimensional gels, eight of the nine subunits of the plastid ATP synthase can be identified by mass spectrometry (Figure 8). Taken together, we could identify all subunits of the plastid ATP synthase in etioplast membranes (Figures 7 and 8).

Immunolocalization studies of freeze-fractured etioplasts uncovered that the $CF_1\alpha$ subunit is almost exclusively found at the stromal site of the inner-envelope membrane (Figure 9). Little gold label can also be detected at membranes found in the etioplast stroma (data not shown). These results demonstrate that the ATP synthase in etiolated lupine cotyledons is present at the inner-envelope membrane. The orientation of the complex allows the formation of the thylakoid system during the etioplast-to-chloroplast transition through a vesicle flow in which the ATP synthase complex is properly orientated (cf. Discussion).

## Discussion

Plant growth and development are dramatically altered in response to cytokinin and abscisic acid (Fedoroff, 2002; Finkelstein and Lynch, 2000; Finkelstein *et al.*, 1998; Grill and Himmelbach, 1998; Haberer and Kieber, 2002; Mok and Mok, 2001; Wu *et al.*, 1997), and transcriptional regulation has been widely investigated (cf. Brandstatter and Kieber, 1998; Busk and Pages, 1998; Hutchison and Kieber, 2002; Sheen, 2002). Our current understanding defines cytokinin action as a multi-step two-component signaling pathway (Hutchison and Kieber, 2002; Hwang and Sheen, 2001; Hwang *et al.*, 2002; Oka *et al.*, 2002; Sheen, 2002), which can be resolved in four major steps: (i) upon cytokinin perception, plasma membrane-bound histidine protein kinases (Inone *et al.*, 2001) initiate a phosphorelay cascade;

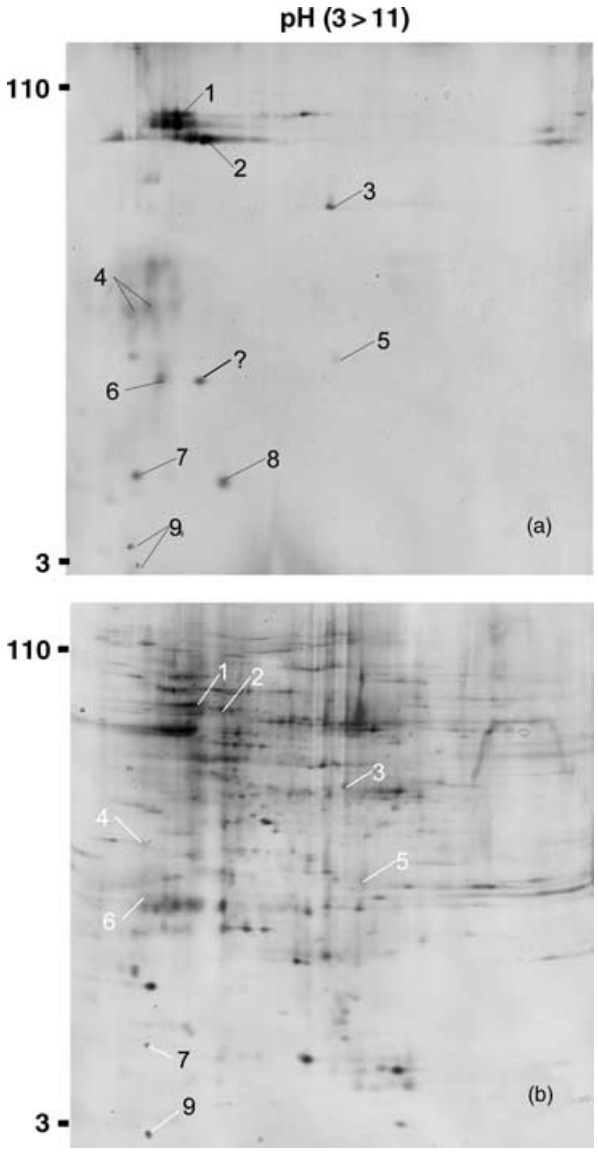


**Figure 8.** The ATP synthase is present in lupine etioplasts.
Two-dimensional gels with protein extracts from purified ATP synthase preparations (a) or membrane preparations of lupine etioplasts (b). Spots relevant for this presentation are indicated. 1, $CF_1\alpha$; 2, $CF_1\beta$; 3, $CF_1\gamma$; 4, $CF_0$IV; 5, $CF_0$I; 6, $CF_1\delta$; 7, $CF_0$II; 8, $CF_1\varepsilon$; 9, $CF_0$III.

(ii) these signals converge at histidine phosphotransfer proteins; (iii) the nuclear translocation of the phosphotransfer proteins causes an activation of B-type response regulator proteins, i.e. transcription factors, which, in turn, activate the transcription of A-type response regulator genes; and (iv) the latter proteins initiate a negative feedback mechanism, which controls the induction of primary cytokinin-responsive genes (Sheen, 2002). While the third step of this model is purely transcriptional, the last step opens the possibility for various control processes operating at the post-transcriptional level, in particular, at the RNA level. This is consistent with the observation that many cytokinin-induced processes cannot be explained exclusively by transcriptional events. Cytokinin and abscisic acid control mRNA stability, rRNA synthesis (Cherepneva *et al.*, 2003; Kukina *et al.*, 1985; Mikulovich *et al.*, 1978), ribosome formation, recruitment of messages into polysomes, polysome degradation (Ananiev *et al.*, 1980; Kliachko *et al.*, 1973), phosphorylation of ribosomal proteins, and post-translational modifications of proteins (Yakovleva *et al.*, 1992). Here, we demonstrate that recruitment of the *AtpC* message into the polyribosome fraction promotes synthesis of the plastid-localized protein (Figure 3) and stimulates ATP synthase accumulation (Figure 7). We used a previously established lupine cotyledon system (Kusnetsov *et al.*, 1994) because the cotyledons continued to develop, respond to phytohormones, and green upon transfer to light during the experimental set-up, although they were excised from the hypocotyls. The specificity of the phytohormone effects could easily be demonstrated by including water controls. Furthermore, phytohormones were taken up by the cotyledons and initiated morphogenetic changes within hours. The huge cotyledons contain large amounts of (poly)ribosomes. Our data suggest that changes in the phytohormone levels in the cotyledons affect the translation efficiency of the available ATP synthase mRNAs, although the exact amount of the physiologically active phytohormone levels are difficult to determine. In general, we found that the overall cytokinin level is low and the abscisic acid level is high in seeds. While the acid level decreases almost linearly within the first few days after germination, the cytokinin level increases up to day 3 and decreases thereafter (Kusnetsov *et al.*, 1994). The physiological relevance of our observations for plant development can only be understood when the physiologically active portion of the phytohormone level is known. Finally, even etioplasts can be isolated in huge amounts from etiolated lupine cotyledons, which allows to compare them after different phytohormone treatments.

Various fusions between the spinach *AtpC* and the bacterial *uidA* gene gave rise to *uidA* messages with different *AtpC* 5′ UTRs (Figure 6). Analysis in transgenic tobacco seedlings clearly demonstrates that the spinach 5′ UTR is responsible and sufficient for the cytokinin-mediated recruitment of the chimeric messages into the polyribosomal fraction (Figure 5). We could also pinpoint nucleotides within the 173 bp long 5′ UTR that are essential for this regulation (Figure 6, M1 and M2). To our knowledge, this is the second plant message for which all identified *cis*-elements involved in such a regulation are located exclusively in the 5′ UTR. The first report describes light-stimulated polyribosome loading of the *uidA* message fused downstream of the spinach *PsaD* 5′ (subunit II of photosystem I reaction center) UTR (Sherameti *et al.*, 2002). In this case, the signal derived from the photosynthetic electron flows in

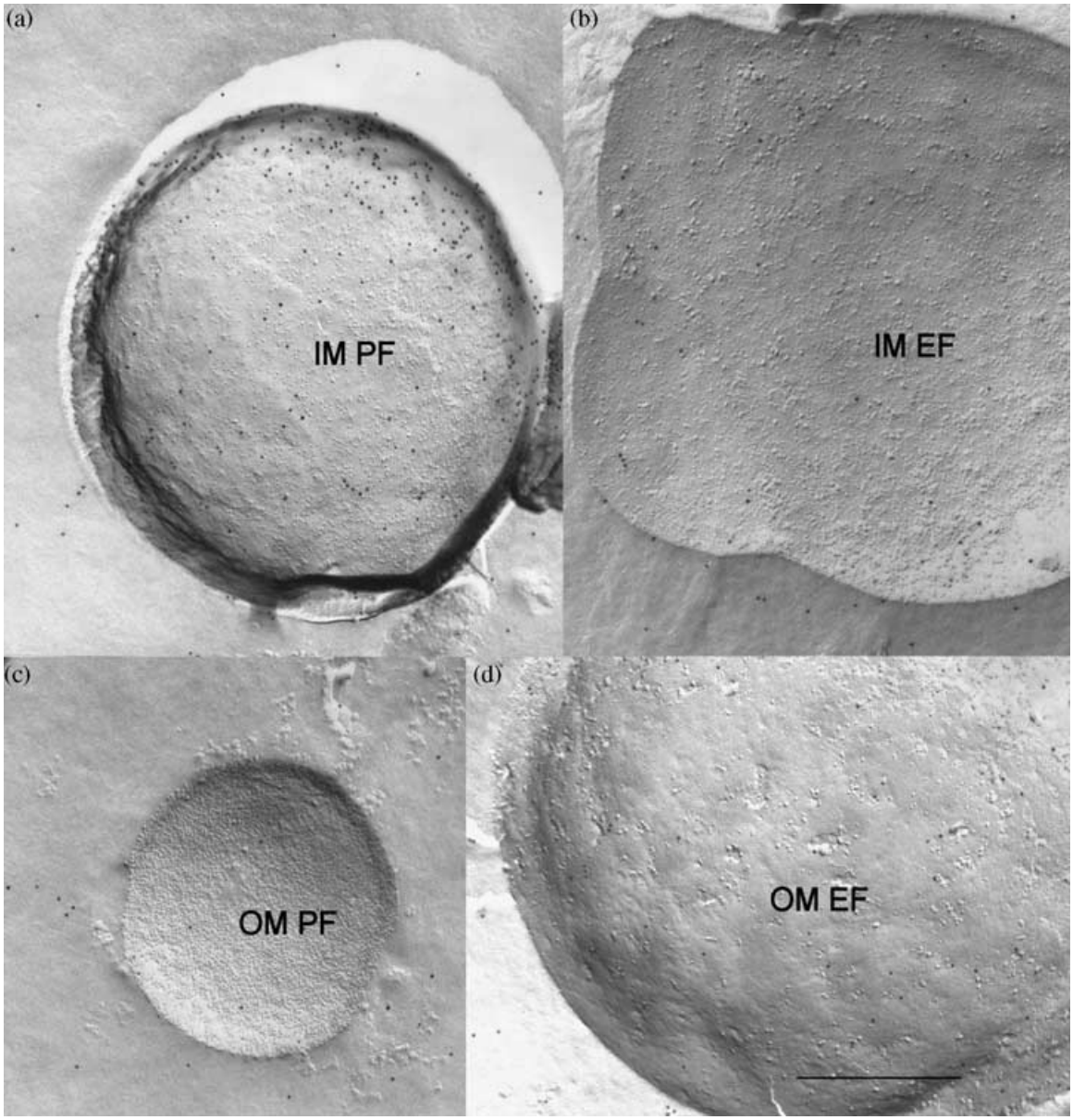


**Figure 9.** Localization of the $CF_1\alpha$ subunit in etioplast membranes by freeze-fracture immunogold labeling.
Protoplasmic fracture faces (PF) can be identified by high numbers of integrated intramembrane protein particles (a,c), in contrast to exoplasmic fracture faces (EF), exhibiting fewer numbers of intramembrane protein particles (b,d). It is known that membranes with protoplasm inside, like the inner-envelope membrane, show PF-faces (IM PF) with convex shape (a) and EF-faces (IM EF) with concave shape (b; Cline *et al.*, 1985). The outer-envelope membrane is an inverted membrane with protoplasm outside, therefore the PF-face of the outer-envelope membrane (OM PF) has concave shape (c) and the EF-face (OM EF) has convex shape (d). Numerous $CF_1\alpha$ subunits, indicating 10-nm gold particles, were found at the PF (stromal site) of the inner-envelope membrane (IM PF) in (a). Very low labeling density of the $CF_1$ subunit was found at the EF of the inner-envelope membrane (IM EF), shown in (b) and on the protoplasmic and exoplasmic fracture faces of the outer-envelope membrane (OM PF and OM EF) in (c) and (d). Bars = 500 nm.

the thylakoid membrane (cf. below). Thus, it appears that the translation efficiency of a message can be regulated in response to different signals.

Using run-on transcription assays with isolated nuclei and the expression of transgenes in tobacco, we have previously shown that sequences upstream of the transcription start site in concert with those coding for the 5′ UTR of *AtpC* are involved in transcription (Bezhani *et al.*, 2001; Bolle *et al.*, 1996a,b; Kusnetsov *et al.*, 1999). Consistent with these results, we detected *AtpC* 5′-UTR-containing messages in all lines in which the gene fusions were transcribed (Figure 6, lane T in all panels). Here, we describe an additional regulatory step which rapidly fine-tunes *AtpC* gene expression by recruitment of the message into the polyribosomal fraction after a course control at the level of transcription (cf. Figure 3).

Polyribosome association is crucial for mRNA stability, and this is one target site for regulation (cf. Abler and Green, 1996; Sullivan and Green, 1993). Often, *cis*-regulatory elements are located at the 5′ end or within the 5′ UTR of the message, and are responsible for the establishment of a secondary structure (Dickey *et al.*, 1998; Petracek and Thompson, 2000; Petracek *et al.*, 1997; Sherameti *et al.*, 2002; Yamamoto *et al.*, 1995). The 5′ UTR of the (γ-glutamylcysteine synthase mRNA, for instance, which is efficiently translated in response to cellular redox signals, is recognized by a protein. Binding of this protein is redox-sensitive and recognizes a secondary structure in the 5′ UTR. Light regulation of the pea *Fed-1* (ferredoxin 1) is caused by differential translation efficiencies of the message, because free messages are more susceptible to degradation than polyribosome-associated messages. The spinach *PsaD* 5′ UTR responds to light and limitations of the photosynthetic electron flow. A rapid association of messages with polyribosomes under stress conditions has also been demonstrated for stress-response proteins. The *AtpC* message provides an example for phytohormone-controlled polyribosome loading. It appears that control of the translation efficiency of individual mRNAs in response to various signals is an efficient and rapid way of a plant to respond and acclimate to environmental changes (cf. Figure 3).

Figure 6 demonstrates that an UC-rich sequence motif located in the 3′ region of the *AtpC* 5′ UTR contributes to cytokinin-mediated polyribosome loading. Databank searches revealed that this sequence is present in many 5′ UTRs of plant genes and, depending on the programs used, can form quite complex secondary structures with neighboring sequences within and outside of 5′ UTRs (data not shown). Thus, a specific involvement of this sequence in the expression of the nuclear-encoded subunits of the ATP synthase is difficult to predict. Hotchkiss and Hollingsworth (1999) showed that spinach chloroplast extracts contain polypeptides that specifically interact with the 5′-UTR of three of the four genes in the large ATP synthase gene cluster. The authors hypothesize that these polypeptides may serve to control the stoichiometry of the ATP synthase subunits or may adjust the abundance of the entire ATP synthase complex in response to environmental or developmental cues. Thus, a coordinated expression of genes in both compartments might be achieved by translational events.

Cytokinin stimulates synthesis and accumulation of the plastid ATP synthase in etioplasts (Figures 7 and 8), which raises the question about the function of this complex in non-photosynthetic organelles and, more specifically, where the complex accumulates when no thylakoids are available. The lupine cotyledons appear to be an excellent model system to study this question because the ATP synthase is present in comparable amounts in etioplasts and chloroplasts (Figure 7). It is also obvious that the fate and the location of the complex must change completely during the transition of an etioplast to a chloroplast. Our data indicate that in lupine etioplasts, the complex assembles in the inner-envelope membrane in an orientation that allows the release of the complex from the envelope membrane by vesicles to generate or join the thylakoid system (Figure 9). Thus, we propose that the assembled ATP synthase complex might be transferred to the thylakoid membrane via vesicle flow, similar to models proposed for other photosystems (Huang *et al.*, 2002; Kroll *et al.*, 2001; Westphal *et al.*, 2001; Zak *et al.*, 2001). Alternatively, the ATP synthase could also be synthesized and be functional in both envelope and thylakoid membranes. The *S*-adenosyl-L-methionine:Mg-protoporphyrin IX methyltransferase is one example of an enzyme that is present in both membranes (Block *et al.*, 2002). The presence of photosynthesis proteins in plasma membrane preparations from *Synechocystis*, including those for the ATP synthase, has also been reported (Huang *et al.*, 2002), and is consistent with the idea that transfer of thylakoid complexes via vesicle flow is a process of ancient phylogenetic origin.

However, besides ATP synthase accumulation in the thylakoid membranes via vesicle flow, it also appears that direct assembly of this complex in plastid membrane systems occurs. It is very well known that some polypeptides of the thylakoid complexes, including those of the ATP synthase (cf. Herrmann *et al.*, 1991), accumulate in etioplasts and other types of non-photosynthetically active plastids, while others do not (cf. Palomares *et al.*, 1993), depending on the protein and the species under study. For instance, little amounts of the subunits of the ATP synthase can be detected in protein extracts from etiolated *Arabidopsis* seedlings, from flowers or roots (unpublished data). These proteins are also not detectable in the inner-envelope membrane of green *Arabidopsis* leaves. Koo and Ohlrogge (2002) isolated plastid inner-envelope membrane proteins from chloroplasts and identified them by mass spectrometry. We could not identify a single ATP synthase subunit in their protein list. This suggests that the ATP synthase complex in green *Arabidopsis* seedlings might assemble directly in the thylakoid membranes without the passage through the inner-envelope membrane. In contrast, ATP synthesis occurs in chromoplasts from *Narcissus pseudonarcissus*, and several subunits of the ATP synthase complex can be detected immunologically (Morstadt *et al.*, 2002). *Narcissus* chromoplasts contain huge amounts of membranes which differ from thylakoids, but are derived from the inner-envelope membrane (Liedvogel *et al.*, 1976). It remains to be determined when and where the ATP synthase is synthesized and which of the two scenarios is involved in ATP synthase biosynthesis during the proliferation of the chromoplast membrane system.

## Experimental procedures

### *Plant growth*

Lupine (*L. luteus* L. cv. Drujnii-165) seeds were germinated on moistened filter paper in the dark for 3 days (25°C). Cotyledons were excised in green safe light and incubated on water for 24 h to diminish the endogenous phytohormone levels. Thereafter, they were transferred to cytokinin ($2.2 \times 10^{-5}$ M), abscisic acid ($7.6 \times 10^{-5}$ M), or water, and kept in darkness (or light, cf. Figure 6) for an additional 24 h. The experimental set-up, effect of phytohormone treatment on the greening process, plastid ultrastructure, pigment composition, development of the thylakoid membrane, accumulation of thylakoid proteins, and expression of photosynthesis genes, as well as determination of the phytohormone concentrations, have been described by Kusnetsov *et al.* (1994). Tobacco (*Nicotiana tabacum* var. Samsun NN) seeds were surface-sterilized, planted on 1/2 Murashige and Skoog (MS) medium supplemented with 2% sucrose, kept in the cold room in darkness for 2 days to synchronize germination before transfer to darkness for 10 days at 22°C. Cotyledons were then harvested in green safe light and further incubated on sucrose-containing Petri dishes supplemented with either nothing (water control), cytokinin ($2.2 \times 10^{-5}$ M), or abscisic acid ($7.6 \times 10^{-5}$ M) for 24 h. Propagation of the tobacco seeds occurred in a greenhouse (day length 16 h at 20°C); for the experiments described here, $F_3$ seeds were used.

### *Gene constructs for tobacco transformation*

The transgenic lines with *AtpC* promoter::*uidA* gene fusions have been described by Bolle *et al.*, (1994, 1996a,b). The genomic sequence of the spinach *AtpC* gene and its environment is deposited in the Databank (X76131). The DNA fragment was cloned into pBI101.2 as a *Sac*I/*Xba*I fragment. The T-DNA region was then transferred to *N. tabacum* var. Samsun NN via *Agrobacterium tumefaciens*. A PCR product specific for the spinach *AtpC* gene was used to confirm the success of the transformation. The two primers amplified 150 bp upstream and 120 bp downstream of the ATG codon. The latter region encoded the plastid-directing transit sequence. This DNA fragment was also used as a spinach *AtpC*-specific probe.

### *Polyribosome analysis, genes, and hybridization conditions*

Polyribosome analysis was performed essentially as described by Davies and Abe (1995) and modified by Dickey *et al.* (1998). A detailed protocol has been described by Sherameti *et al.* (2002). In brief, a protein fraction enriched in polyribosomes was isolated from the cotyledons. RNA was isolated from a small portion of this fraction to confirm that the overall transcript levels for *AtpC*, *AtpD*, and *AtpG* were comparable in each preparation, irrespective of the treatment of the cotyledons. 1 ml of the residual fraction was loaded onto a 10-ml sucrose gradient. After centrifugation, 1-ml fractions of the gradient were harvested by puncturing the bottom of the tube. The sucrose gradient fractions were collected in tubes with phenol–chloroform. After RNA extraction, hybridization under stringent conditions (Sambrook *et al.*, 1989) was performed, either with ESTs from *Arabidopsis* (*AtpC*, *AtpD*, *AtpG*, *Tub*; cf. Sherameti *et al.*, 2002), with the above described lupine genes for ribosomal proteins, or with gene-specific fragments. A spinach *AtpC*-specific probe was obtained by PCR from the region −150/+120, relative to the ATG codon (see above). An *uidA*-specific probe was isolated as a *Sma*I/*Sac*I fragment from the *uidA* gene cloned in pBI101.2 (Jefferson *et al.*, 1987). The hybridization signals were detected by a phosphorimager (Storm Model 802; Amersham Biosciences, Freiburg, Germany). Genomic DNA from *L. luteus* was used as template for the polymerase chain reaction to isolate *rps16*, *rpl13a*, and *rpl30* (Cherepneva *et al.*, 2003). The DNA fragments were cloned into the pGEM-T Easy Vector (Promega, Mannheim, Germany), and were sequenced.

### *Quantitative PCR*

An amount of 0.2 μg of RNA was used for cDNA synthesis with 5 ng of an oligo(dT)-15 primer (Promega, Heidelberg, Germany) and water in a final volume of 21 μl. After incubation at 65°C for 10 min and 5 min on ice, the reaction was started by the addition of 2.5 μl 400 mM Tris–HCl (pH 8.3), 2.5 μl 400 mM KCl, 1 μl 300 mM $MgCl_2$, 5 μl 100 mM DTT, 4 μl 5 mM dNTPs (deoxynucleotide triphosphates), 14 μl $H_2O$, and 16 units AMV (arian myeloblastosis virus) RT (Böhringer, Mannheim, Gemany). cDNA synthesis occurred at 42°C for 1 h. The final reaction mix of 40 μl was used for the quantitative PCR following the protocol of White *et al.* (1992). PCR parameters and the amount of cDNA were optimized such that the amplification was linear with regard to the reaction products and the number of PCR cycles. The reaction mixture contained 200 nM of each primer, 19 mM Tris–HCl (pH 8.3), 1 mM $MgCl_2$, 50 mM KCl, and 1 mg $ml^{-1}$ gelatine. The reaction was started by adding a master mix to the respective cDNAs. A negative control without cDNA was included in the experiments. Between 17 (minimum) and 29 (maximum) cycles were used for each fraction of the gradients depending on the amount of message. The two oligonucleotides (5′-GCAGACTATCCCGCCGGGAATGG-3′ and 5′-GCGTGGTCGTGCACCATCAGCACG-3′) were designed to amplify a 500 bp long cDNA fragment from the *uidA* message and a 300 bp long internal standard. The standard, generated from the 500 bp *uidA* fragment, was purified from agarose gels, and was digested with *Eco*RV to give three fragments. They were ligated overnight, and the ligation product lacking the internal *Eco*RV fragment was re-amplified using the same primers. The truncated *uidA* fragment of approximately 300 bp was purified by successive cycles of PCR amplification and agarose gel electrophoresis. 2 fg of this fragment was found to be optimal for co-amplification, and was included in all reactions.

### *Isolation of etioplast membranes from* L. luteus *cotyledons, purification of the ATP synthase*

The cotyledons were collected in green safe light in the cold room and homogenized in 3 volumes (w/v) of homogenization buffer (50 mM Tris–HCl (pH 8.0), 300 mM saccharose, 10 mM NaCl, 0.1% β-mercaptoethanol). After filtration through an 80-μm gaze (1×), Miracloth (1×), and a 20-μm gaze (2×), the filtrate was centrifuged at 5000 ***g*** for 6 min. The pellet was washed once in homogenization buffer. Ultimately, the etioplasts in homogenization buffer were layered onto a linear 30–70% sucrose gradient (20 mM Tris–HCl (pH 8.0), 10 mM $MgCl_2$) and centrifuged at 23 000 ***g*** for 45 min. The etioplast band was harvested and re-centrifugated on a linear 45–60% sucrose gradient. The etioplast band was eluted again, diluted twofold with sucrose-free buffer, and then pelleted at 10 000 ***g*** for 30 min. The etioplast pellet was then re-suspended either in 10 mM MOPS (3-(*N*-morpholino)propanesulfonic acid)

(pH 8.0), 300 mM sucrose, 10 mM NaCl, 10 mM $MgCl_2$ for electron microscopy, or in lysis buffer (10 mM Tris–HCl (pH 8.0), 200 mM NaCl). The etioplasts were briefly treated with a microdismembrator (two times for 2 sec), then stirred on ice for 30 min before the soluble proteins were separated from the membrane-associated proteins by centrifugation (10 000 ***g*** for 30 min). The pellet was washed once with a 100-fold excess of lysis buffer and finally with 0.1 M sodium carbonate to remove loosely attached proteins.

The plastid ATP synthase was solubilized from thylakoid membranes of 7-day-old white-light-grown lupine seedlings by sucrose gradient centrifugation. Fractions with the purified ATP synthase complex were identified by SDS–polyacrylamide gel electrophoresis (PAGE). The complex in the sucrose fraction was diluted two times with buffer and pelleted by centrifugation.

### *Preparation of whole cell protein extracts, SDS–PAGE, Western analysis*

A crude protein extract was obtained by grinding seven cotyledons, frozen in liquid nitrogen, in 5 ml extraction buffer (100 mM Tris–HCl (pH 7.5), 10 mM $MgCl_2$). Soluble and membrane-associated proteins were separated by centrifugation (20 min at 4°C, 28 000 ***g***). The protein concentration in the supernatant with the soluble proteins was determined by Lowry (1951), the solution was adjusted to 2.2% (w/v) SDS, and boiled for 10 min. The pellet of the centrifugation was re-suspended in 5 ml of extraction buffer (100 mM Tris–HCl (pH 7.5), 10 mM $MgCl_2$) in the presence of 2.2% SDS and 5 M PMSF (phenylmethylsulfonylfluoride), and dissolved by gently shaking at 70°C for 10 min followed by 37°C for 30 min. The solution was then clarified by centrifugation (20 min at 4°C, 28 000 ***g***) and an aliquot was used for protein determination. An equal amount of protein from both fractions (40 g per lane) was loaded on denaturing polyacrylamide gels using the system of Schägger and von Jagow (1987). Western analysis was performed with monospecific antibodies as described by Bolle *et al.*, (1992) and Kusnetsov *et al.* (1999).

### In vivo *labeling of proteins*

Two hours before harvest, one excised cotyledon was submersed into a $^{35}$S-methionine containing half-strength MS medium (100 μCi/2 ml medium). Proteins were extracted as described above.

Aliquots of the protein extracts corresponding to 100 000 c.p.m. (35–80 μl) were used for immunoprecipitations. The protein extracts were diluted with IP (immunoprecipitation) buffer (10 mM Tris–HCl (pH 8.0), 150 mM NaCl, 0.1% Triton X-100) to 1.3 ml, and 0.5 μg of purified AtpC protein fused in-frame to the N-terminal 6× His-affinity tag was added to the solution. Immunoprecipitation was performed with 9 μl of purified antibody solution. Prior to experimentation, it was ensured that the amount of antibodies was not limiting for the precipitation (cf. Figure 3d). The solution was incubated at room temperature for 1 h and kept at 4°C overnight. The antigen–antibody conjugate was then precipitated with Protein A by centrifugation (2 min, 10 000 ***g***), and the pellet washed four times with IP buffer. The proteins were solubilized from the complex by adding sample buffer (Schägger and von Jagow, 1987) and by boiling for 5 min. After gel electrophoresis, the radiolabeled bands were visualized with a phosphorimager.

### *Preparation of antibodies against* Arabidopsis *AtpC*

For generation of antibodies against AtpC, two protein fusions in *Escherichia coli* were generated. The first protein contained an AtpC segment fused in-frame to the N-terminal 6× His-affinity tag of pET15. After isolation of the protein from inclusion bodies, it was purified on a Ni–NTA resin matrix. Aliquots of this protein preparation, representing 0.5 μg protein, were also included into the immunoprecipitation reactions. The same AtpC fragment was fused in-frame to the glutathione-*S*-transferase sequence (GST-Hcf101) of pGEX-4T-1 and the protein was purified from inclusion bodies. This protein was used for antibody production. The His-tagged fusion protein was separated on polyacrylamide gels, transferred to nitrocellulose membranes, and the prominent band was cut out from the membrane after visualization with Ponceau stain. The filter was blocked and the antibodies raised against the GST-AtpC fusion protein were purified on the immobilized His-tagged protein. Antibodies were raised in rabbits.

### *Two-dimensional gel electrophoresis, preparation of proteins*

An amount of 180 μg of protein in 100 μl of extraction buffer was precipitated with methanol, dried, and re-suspended in 380 μl of sample buffer (8 M urea, 2 M thiourea, 30 mM dithioereitrol, 4% (w/v) CHAPS (3-[(3-cholamidopropyl)dimethylammonio]-propane sulfonate), 20 mM Tris base, 0.5% bromphenol blue, 0.5% isoelectric pH gradient (IPG) buffer (pH 3–10; Amersham Pharmacia, Freiburg, Germany), 0.05% dodecyl-β-D-maltoside). An amount of 350 μl of the supernatant was added to 1.75 ml 0.5% (v/v) IPG buffer for isoelectric focusing (Amershan Pharmacia). For the second dimension, the gel system of Schägger and von Jagow (1987) was used. Gels were stained with silver.

### *Mass spectrometry, preparation of the samples by tryptic digestions*

Silver-stained gel spots were excised, and the proteins were extracted into 500 μl 50 mM ammonium bicarbonate, supplemented with 60 ng $\mu l^{-1}$ trypsin. After lyophilization, the pellet was re-suspended in 5 μl of water/acetonitrile/formic acid (95 : 5 : 0.1) prior to LC–MS analysis. Peptide analyses, analyte sampling, chromatography, and acquisition of data were performed on a LC (Famos-Ultimate; LC-Packings, Amsterdam, the Netherlands) coupled with an LCQ Deca XP ITMS (Thermoelectron, San Jose, CA, USA) according to manufacturer's instructions.

### *Freeze-fracture electron microscopy*

Small amounts of the organelle suspension were enclosed between two 0.1-mm copper profiles as used for the sandwich double-replica technique. The sandwiches were rapidly frozen by plunging them into liquid propane, and cooled by liquid nitrogen. Freeze-fracturing was performed in a BAF400T (BAL-TEC; Balzers, Lichtenstein) freeze-fracture unit at −150°C using a double-replica stage. The fractured samples were shadowed without etching with 2–2.5 nm Pt/C at an angle of 35°.

### *Immunoelectron microscopy*

Prior to freeze-fracture immunogold labeling, replica were incubated for 16–20 h in digesting solution (10 mM Tris (pH 8.3), containing 2.5% (w/v) SDS and 30 mM sucrose) according to Fujimoto (1995). The replica were subsequently washed four times in NaCl/phosphate buffer (75 mM NaCl, 12 mM $NaH_2PO_4$, 67 mM $Na_2HPO_4$ (pH 7.2)) and incubated for 30 min in NaCl/phosphate buffer with

1% (w/v) BSA. For immunogold labeling, the replica were placed on a drop of 0.5% BSA in NaCl/phosphate buffer, then transferred on a drop of a 1 : 50 diluted solution of the $CF_1\alpha$ antibody in NaCl/phosphate buffer with 0.5% BSA, and incubated for 1 h. After four washing steps with NaCl/phosphate buffer, replica were incubated for 1 h in NaCl/phosphate buffer containing 0.5% BSA and 1 : 50 diluted secondary gold-conjugated antibody (gold anti-(rabbit-IgG) Ig with 10 nm gold; British Biocell International, Cardiff, UK). The replica were finally rinsed several times with NaCl/phosphate buffer, fixed with 0.5% (w/v) glutaraldehyde in NaCl/phosphate buffer for 10 min at room temperature, washed four times in distilled water, and picked onto Formvar-coated grids for viewing in the EM 902 electron microscope (Zeiss, Oberkochen, Germany). All freeze-fracture micrographs were mounted with direction of shadowing from bottom to top.

## Acknowledgements

Work was supported by the German Research Foundation (SFB 604), the Russian Foundation for Basic Research (01-04-48036), the Friedrich-Schiller-University Jena, and the DAAD (Bonn).

## References

**Abler, M. and Green, P.J.** (1996) Control of mRNA stability in higher plants. *Plant Mol. Biol.* **32**, 63–78.

**Abrahams, J.P., Leslie, A.G.W., Lutter, R. and Walker, J.E.** (1994) Structure at 2.8 A resolution of $F_1$-ATPase from bovine heart mitochondria. *Nature*, **370**, 621–628.

**Ananiev, E.D., Shakirova, F.M., Klyachko, N.L. and Kulaeva, O.N.** (1980) Effect of cytokinin on polyribosome formation from pre-existing mRNA and ribosomes. *Dokl. Akad. Nauk SSSR*, **255**, 508–510 (in Russian).

**Bezhani, S., Sherameti, I., Pfannschmidt, T. and Oelmüller, R.** (2001) A repressor with similarities to pro- and eukaryotic DNA helicases controls the assembly of the CAAT-box binding complex at a photosynthesis gene promoter. *J. Biol. Chem.* **276**, 23785–23789.

**Block, M.A., Tewari, A.K., Albrieux, C., Marechal, E. and Joyard, J.** (2002) The plant *S*-adenosyl-L-methionine: Mg-protoporphyrin IX methyltransferase is located in both envelope and thylakoid membranes. *Eur. J. Biochem.* **269**, 240–248.

**Bolle, C., Kusnetsov, V., Michl, D., Cai, D., Klösgen, R.-B., Oelmüller, R. and Herrmann, R.G.** (1992) The genes for the three nuclear-coded subunits of chloroplast ATP synthases: characterization of the promoters from the single-copy genes *atpC* and *atpD* from spinach. In *Research in Photosynthesis*, **Vol. III** (Murata, N., ed.). Dordrecht, Boston, London: Kluwer Academic Publishers, pp. 377–380.

**Bolle, C., Sopory, S., Lübberstedt, Th, Herrmann, R.G. and Oelmüller, R.** (1994) Segments encoding 5′-untranslated leader sequences of genes for thylakoid proteins contain *cis*-elements essential for transcription. *Plant J.* **6**, 513–523.

**Bolle, C., Kusnetsov, V.V., Herrmann, R.G. and Oelmüller, R.** (1996a) The spinach *AtpC* and *AtpD* promoters contain important elements for the regulated expression in the vicinity of their transcription start sites. *Plant J.* **9**, 21–30.

**Bolle, C., Herrmann, R.G. and Oelmüller, R.** (1996b) Different sequences for 5′-untranslated leaders of nuclear genes for plastid proteins affect the expression of the β-glucuronidase gene. *Plant Mol. Biol.* **32**, 861–868.

**Boyer, P.D.** (1997) The ATP synthase – a splendid molecular machine. *Ann. Rev. Biochem.* **66**, 717–749.

**Brandstatter, I. and Kieber, J.J.** (1998) Two genes with similarity to bacterial response regulators are rapidly and specifically induced by cytokinin in *Arabidopsis*. *Plant Cell*, **10**, 1009–1019.

**Busk, P.K. and Pages, M.** (1998) Regulation of abscisic acid-induced transcription. *Plant Mol. Biol.* **37**, 425–435.

**Cherepneva, G.N., Schmidt, K.-H., Kulaeva, O.N., Oelmüller, R. and Kusnetsov, V.V.** (2003) Expression of the ribosomal proteins S14, S16, L13a and L30 is regulated by cytokinin and abscisic acid. Implication of the involvement of phytohormones in translational processes. *Plant Sci.* **165**, 925–932.

**Cline, K., Keegstra, K. and Staehelin, L.A.** (1985) Freeze-fracture electron microscopic analysis of ultrarapidly frozen envelope membranes of intact chloroplasts and after purification. *Protoplasma*, **125**, 111–123.

**Cross, R.L. and Duncan, T.M.** (1996) Subunit rotation in $F_0F_1$-ATP-synthases as a means of coupling proton transport through $F_0$ to the binding changes in $F_1$. *J. Bioenerg. Biomembr.* **28**, 403–408.

**Davies, E. and Abe, S.** (1995) Methods for isolation and analysis of polyribosomes. In *Methods in Cell Biology* (Galbraith D.W., Bourque D.P. and Bohnert H.J., eds). San Diego, CA: Academic Press, pp. 209–222.

**Dickey, L.F., Petracek, M.E., Nguyen, T.-T., Hansen, E.R. and Thompson, W.F.** (1998) Light regulation of *Fed-A* mRNA requires an element in the 5′ untranslated region and correlates with differential polyribosome association. *Plant Cell*, **10**, 475–484.

**Fedoroff, N.V.** (2002) Cross-talk in abscisic acid signaling. *Sci. STKE* **140**, RE10.

**Finkelstein, R.R. and Lynch, T.J.** (2000) The *Arabidopsis* abscisic acid response gene *ABI5* encodes a basic leucine zipper transcription factor. *Plant Cell*, **12**, 599–609.

**Finkelstein, R.R., Wang, M.L., Lynch, T.J., Rao, S. and Goodman, H.M.** (1998) The *Arabidopsis* abscisic acid response locus ABI4 encodes an APETALA2 domain protein. *Plant Cell*, **10**, 1043–1054.

**Fujimoto, K.** (1995) Freeze-fracture replica electron microscopy combined with SDS digestion for cytochemical labelling of integral membrane proteins. Application of the immunogold labelling of intercellular junction complexes. *J. Cell Sci.* **108**, 558–568.

**Grill, E. and Himmelbach, A.** (1998) ABA signal transduction. *Curr. Opin. Plant Biol.* **1**, 412–418.

**Haberer, G. and Kieber, J.J.** (2002) Cytokinins. New insights into a classic phytohormone. *Plant Physiol.* **128**, 354–362.

**Hansen, E.R., Petracek, M.E., Dickey, L.F. and Thompson, W.F.** (2001) The 5′ end of the pea ferredoxin-1 mRNA mediates rapid and reversible light-directed changes in translation in tobacco. *Plant Physiol.* **125**, 770–778.

**Herrmann, R.G., Oelmüller, R., Bichler, J., Schneiderbauer, A., Steppuhn, J., Wedel, N., Tyagi, A.K. and Westhoff, P.** (1991) The thylakoid membrane of higher plants: genes, their expression and interaction. In *Plant Molecular Biology* **Vol. 2** (Herrmann, R.G. and Larkins, B.A., eds). New York: Plenum Press, pp. 411–427.

**Hotchkiss, T.L. and Hollingsworth, M.J.** (1999) ATP synthase 5′ untranslated regions are specifically bound by chloroplast polypeptides. *Curr. Genet.* **35**, 512–520.

**Huang, F., Parmry, I., Nilsson, F., Persson, A.L., Pakrasi, H.B., Andersson, B. and Norling, B.** (2002) Proteomics of *Synechocystis* sp. strain PCC 6803. *Mol. Cell. Proteomics*, **1** (12), 956–966.

**Hutchison, C. and Kieber, J.J.** (2002) Cytokinin signaling in *Arabidopsis*. *Plant Cell*, **14**, S47–S59.

**Hwang, I. and Sheen, J.** (2001) Two-component circuitry in *Arabidopsis* cytokinin signal transduction. *Nature*, **413**, 383–389.

**Hwang, I., Chen, H.-C. and Sheen, J.** (2002) Two component signal transduction pathways in *Arabidopsis*. *Plant Physiol.* **129**, 500–515.

**Inone, T., Higuchi, M., Hashimoto, Y., Seki, M., Kobayashi, M., Kato, T., Tabata, S., Shinozaki, K. and Kakimoto, T.** (2001) Identification of CRE1 as a cytokinin receptor from *Arabidopsis*. *Nature*, **409**, 1060–1063.

**Jagendorf, A.T. and Uribe, E.** (1966) ATP formation caused by acid-base transition of spinach chloroplasts. *Proc. Natl. Acad. Sci. USA*, **55**, 170–177.

**Jefferson, R.A., Kavanagh, T.A. and Bevan, M.W.** (1987) GUS-fusion: β-glucuronidase as a sensitive and versatile gene fusion marker in higher plants. *EMBO J.* **6**, 3901–3907.

**Junge, W., Lill, H. and Engelbrecht, S.** (1997) ATP synthase: an electrochemical transducer with rotatory mechanics. *Trends Biochem. Sci.* **22**, 420–423.

**Kliachko, N.L., Yakovleva, L.A. and Kulaeva, O.N.** (1973) Activity of protein synthesizing system of isolated gourd cotyledons *in vivo* and effect on its 6-benzylaminopurine. *Fiziol. Rastenii (Moscow)*, **20**, 1219–1223.

**Koo, A.J.K. and Ohlrogge, J.B.** (2002) The predicted candidates of *Arabidopsis* plastid inner envelope membrane proteins and their expression profiles. *Plant Physiol.* **130**, 823–836.

**Kroll, D., Meierhoff, K., Bechtold, N., Kinoshita, M., Westphal, S., Vothknecht, U.C., Soll, J. and Westhoff, P.** (2001) *VIPP1*, a nuclear gene of *Arabiopsis thaliana*, essential for thylakoid membrane formation. *Proc. Natl. Acad. Sci. USA*, **98**, 4238–4242.

**Kukina, I.M., Mikulovich, T.P. and Kulaeva, O.N.** (1985) Interaction of abscisic acid and cytokinin in the control of ribosomal RNA biosynthesis in plastids and cytoplasm from detached pumpkin cotyledons. *Fiziol. Rast. (Sov. Plant Physiol. Engl. Transl. Moscow)*, **32**, 298–308.

**Kusnetsov, V.V., Oelmüller, R., Sarwat, M.I., Porfirora, S.A., Cherepneva, G.N., Herrmann, R.G. and Kulaeva, O.N.** (1994) Cytokinins, abscisic acid and light affect accumulation of chloroplast proteins in *Lupinus luteus* cotyledons without notable effect on steady-state mRNA levels. Specific protein response to light/phytohormone interaction. *Planta*, **194**, 318–327.

**Kusnetsov, V.V., Oelmüller, R., Makeev, A.V., Cherepneva, G.N., Romanko, E.G., Selivankina, S.Y., Mokronosov, A.T., Herrmann, R.G. and Kuleava, O.N.** (1996) Cytokinin and abscisic acid in regulation of chloroplast protein gene expression and photosynthetic activity. In *Plant Hormone Signal Perception and Transduction* (Smith, A.R., Berry, A.W., Harpham, N.V.J., Moshkov, I.E., Novikova, G.V., Kuleava, O.N. and Hall, M.A., eds). Dordrecht: Kluwer Academic Publishers, pp. 109–118.

**Kusnetsov, V., Herrmann, R.G., Kulaeva, O.N. and Oelmüller, R.** (1998) Cytokinin stimulates and abscissic acid inhibits greening of etiolated *Lupinus luteus* cotyledons by affecting the expression of the light-sensitive protochlorophyllide oxidoreductase. *Mol. Gen. Genet.* **259**, 21–28.

**Kusnetsov, V., Landsberger, M., Meurer, J. and Oelmüller, R.** (1999) The assembly of the CAAT-box binding complex at a photosynthesis gene promoter is regulated by light, cytokinin and the stage of the plastids. *J. Biol. Chem.* **274**, 36009–36014.

**Liedvogel, B., Sitte, P. and Falk, H.** (1976) Chromoplasts in the daffodil: fine structure and chemistry. *Cytobiol.* **12**, 155–174.

**Ling, J., Wells, D.R., Tanguay, R.L., Dickey, L.F., Thompson, W.F. and Gallie, D.R.** (2000) Heat shock protein HSP101 binds to the *Fed-1* internal light regulatory element and mediates its high translational activity. *Plant Cell*, **12**, 1213–1227.

**Lowry, O.H., Rosebrough, N.J., Farr, A.L. and Randall, R.J.** (1951) Protein measurement with the folin reagent. *J. Biol. Chem.* **193**, 265–275.

**Mikulovich, T.P., Wollgiehn, R., Khokhlova, W.A., Neumann, D. and Kulaeva, O.N.** (1978) Synthesis of plastid and cytoplasmic ribosomal RNAs in isolated pumpkin cotyledons. Effect of cytokinin and light. *Biochem. Physiol. Pflanz.* **172**, 101–110.

**Mok, D.W. and Mok, M.C.** (2001) Cytokinin metabolism and accumulation. *Annu. Rev. Plant Physiol. Plant. Mol. Biol.* **52**, 89–118.

**Morstadt, L., Gräber, P., de Pascalis, L., Kleining, H., Speth, V. and Beyer, P.** (2002) Chemiosmotic ATP synthesis in photosynthetically inactive chromoplasts from *Narcissus pseudonarcissus* L. linked to a redox pathway potentially also involved in carotene desaturation. *Planta*, **215**, 134–140.

**Murashige, T. and Skoog, F.** (1962) A revised medium for rapid growth and bioassays with tobacco tissue cultures. *Physiol. Plant.* **15**, 473–497.

**Noji, H., Yasuda, R., Kinosita, K., Jr and Yoshida, M.** (1997) Direct observation of the rotation of $F_1$-ATPase. *Nature*, **386**, 299–302.

**Oelmüller, R., Schneiderbauer, A., Herrmann, R.G. and Kloppstech, K.** (1995) The steady-state mRNA levels for thylakoid proteins exhibit a coordinated diurnal regulation. *Mol. Gen. Genet.* **246**, 478–484.

**Oka, A., Sakai, H. and Iwakoshi, S.** (2002) His-Asp phosphorelay signal transduction in higher plants: receptors and response regulators for cytokinin signalling in *Arabidopsis thaliana*. *Genes Genet. Syst.* **77**, 383–391.

**Palomares, R., Herrmann, R.G. and Oelmüller, R.** (1993) Post-transcriptional and post-translational regulatory steps are crucial in controlling the appearance and stability of thylakoid polypeptides during the transition of etiolated tobacco seedlings to white light. *Eur. J. Biochem.* **217**, 345–352.

**Petracek, M.E. and Thompson, W.F.** (2000) Post-transcriptional light regulation of nuclear-encoded genes. *Genet. Eng.* **22**, 1–10.

**Petracek, M.E., Dickey, L.F., Huber, S.C. and Thompson, W.F.** (1997) Light-regulated changes in abundance and polysome association of ferredoxin mRNA are dependent on photosynthesis. *Plant Cell*, **9**, 2291–2300.

**Petracek, M.E., Dickey, L.F., Nguyen, T.-T., Gatz, C., Sowinski, D.A., Allen, G.C. and Thompson, W.F.** (1998) Ferredoxin-1 mRNA is destabilized by changes in photosynthetic electron transport. *Proc. Natl. Acad. Sci. USA*, **95**, 9009–9013.

**Petracek, M.E., Nuygen, T., Thompson, W.F. and Dickey, L.F.** (2000) Premature termination codons destabilize ferredoxin-1 mRNA when ferredoxin-1 is translated. *Plant J.* **21**, 563–569.

**Sabbert, D., Engelbrecht, S. and Junge, W.** (1996) Intersubunit rotation in active F-ATPase. *Nature*, **381**, 623–625.

**Sabbert, D., Engelbrecht, S. and Junge, W.** (1997) Functional and idling rotatory motion within $F_1$-ATPase. *Proc. Natl. Acad. Sci. USA*, **94**, 4401–4405.

**Sambrook, J., Fritsch, E.F. and Maniatis, T.** (1989) *Molecular Cloning: a Laboratory Manual.* Cold Spring Harbour, NY: Cold Spring Harbour Laboratory Press.

**Schägger, H. and von Jagow, G.** (1987) Tricine-sodium dodecyl sulfate-polyacrylamide gel electrophoresis for the separation of proteins in the range from 1 to 100 kDa. *Anal. Biochem.* **166**, 368–379.

**Sheen, J.** (2002) Phosphorelay and transcription control in cytokinin signal transduction. *Science*, **296**, 1650–1652.

**Sherameti, I., Nakamura, M., Yoshiharu, Y.Y., Pfannschmidt, Th., Obokata, J. and Oelmüller, R.** (2002) Polyribosome loading of spinach mRNAs for photosystem I subunits is controlled by photosynthetic electron transport. *Plant J.* **32**, 631–639.

**Sullivan, M.L. and Green, P.J.** (1993) Post-transcriptional regulation of nuclear-encoded genes in higher plants – the roles of

messenger RNA stability and translation. *Plant Mol. Biol.* **23**, 1091–1104.

**Westphal, S., Heins, L., Soll, J. and Vothknecht, U.C.** (2001) *Vipp1* deletion mutant of *Synechocystis*: a connection between bacterial phage shock and thylakoid biogenesis? *Proc. Natl. Acad. Sci. USA*, **98**, 42423–44248.

**White, M.J., Fristensky, W., Falconet, D., Childs, L.C., Watson, J.C., Alexander, L., Roe, B.A. and Thompson, W.F.** (1992) Expression of the chlorophyll *a/b*-protein multigene family in pea (*Pisum sativum* L.). *Planta*, **188**, 190–198.

**Wu, Y., Kuzma, J., Marechal, E., Graeff, R., Lee, H.C., Foster, R. and Chua, N.-H.** (1997) Abscisic acid signaling through cyclic ADP-ribose in plants. *Science*, **278**, 2126–2130.

**Yakovleva, L.A., Klueva, N.Y. and Kulaeva, O.N.** (1992) Phosphorylation of ribosome proteins as a mechanism of phytohormone regulation of protein synthesis in plants. In *Physiology and Biochemistry of Cytokinins in Plants* (Kaminek M., Molk D.W.S. and Zazimalova E., eds). The Hague, the Netherlands: The Hague Academic Press, pp. 169–172.

**Yamamoto, Y.Y., Tsuji, H. and Obokata, J.** (1995) 5′-leader of a photosystem I gene in *Nicotiana sylvestris*, *psaDb*, contains a translational enhancer. *J. Biol. Chem.* **270**, 12466–12470.

**Zak, E., Norling, B., Maitra, R., Huang, F., Andersson, B. and Pakrasi, H.B.** (2001) The initial steps of the biogenesis of cyanobacterial photosystems occur in plasma membranes. *Proc. Natl. Acad. Sci. USA*, **98**, 13443–13448.